



UNIVERSITY OF LEEDS

This is a repository copy of *Upgrading agro-pellets by torrefaction and co-pelletization process using food waste as a pellet binder*.

White Rose Research Online URL for this paper:

<https://eprints.whiterose.ac.uk/188224/>

Version: Accepted Version

Article:

Guo, F, Chen, J, He, Y et al. (4 more authors) (2022) Upgrading agro-pellets by torrefaction and co-pelletization process using food waste as a pellet binder. *Renewable Energy*, 191. pp. 213-224. ISSN 0960-1481

<https://doi.org/10.1016/j.renene.2022.04.012>

© 2022, Elsevier. This manuscript version is made available under the CC-BY-NC-ND 4.0 license <http://creativecommons.org/licenses/by-nc-nd/4.0/>.

Reuse

This article is distributed under the terms of the Creative Commons Attribution-NonCommercial-NoDerivs (CC BY-NC-ND) licence. This licence only allows you to download this work and share it with others as long as you credit the authors, but you can't change the article in any way or use it commercially. More information and the full terms of the licence here: <https://creativecommons.org/licenses/>

Takedown

If you consider content in White Rose Research Online to be in breach of UK law, please notify us by emailing eprints@whiterose.ac.uk including the URL of the record and the reason for the withdrawal request.



eprints@whiterose.ac.uk
<https://eprints.whiterose.ac.uk/>

1 **Upgrading argo-pellets by torrefaction and co-pelletization**

2 **process using food waste as a pellet binder**

3 Feihong Guo¹, Jun Chen², Yi He³, Jabbar Gardy³, Yahui Sun¹, Jingyu Jiang¹, Xiaoxiang Jiang^{1*}

4 ¹Engineering Laboratory for Energy System Process Conversion and Emission Control Technology of
5 Jiangsu Province, School of Energy and Mechanical Engineering, Nanjing Normal University, Nanjing,
6 210042, China

7 ² Rural Technology Service Center of Jiangsu Association of Science and Technology, Nanjing, 210019,
8 China

9 ³ School of Chemical and Process Engineering, Faculty of Engineering and Physical Sciences, University
10 of Leeds, Leeds, LS2 9DT, UK

12 **ABSTRACT:**

13 This work presents a study on the properties of upgraded argo-pellets produced
14 by torrefaction and co-pelletization process, where starch-rich food waste was used as
15 a pellet binder. The impact of blending coal cutting waste (CCW), torrefaction pre-
16 treatment and the use of starch binder on the mechanical properties of argo-pellets
17 were examined. The resulting physical properties of argo-pellets were significantly
18 improved. Thermal decomposition of corn straw (CS) can be divided into three stages.
19 Co-pelleting with a small amount of CCW promote the combustion of CS, showing an
20 improved thermodynamic characteristic of torrefied corn straw (TCS). Torrefaction
21 reduces the difference of heat distribution, improving the adaptability of pellet fuel in
22 operation. Both co-pelletization and torrefaction processes lead to reduced
23 concentrations of NO_x and SO₂, increased calorific value of fuel and elevated CO₂
24 emission per unit mass, which are conducive to pollutants reduction and
25 thermodynamic qualities of argo-pellets. Moreover, life cycle assessment (LCA)
26 analysis indicated that more energy input was required for co-pelletization and
27 torrefaction pre-treatment, consequently leading to an enhanced energy return ratio.

28
29 **KEYWORDS:** Argo-pellets, torrefaction, co-pelletization, starch binder, life cycle
30 analysis, energy

32 1. INTRODUCTION

33 China has become the world's largest emitter of carbon, nitrogen and sulphur
34 oxides due to its over-reliance on coal [1], which calls for the development of
35 alternative energy conversion from biomass. This is further promoted by a series of
36 policies made recently in China [2]. The wastes in agricultural production and wood
37 industry are the main source of biomass [3]; however, direct utilization of biomass
38 feedstock is often not practical, this is due to its low energy density, unstable
39 combustion and difficulties in storage and transportation while biomass pellet
40 presents a much higher bulk density, making it suitable for long distance
41 transportation and storage. Together with its high calorific value in combustion [4, 5]
42 and sustainable characteristics of biomass, application of biomass pellet is at the
43 center of both scientific research and industrial practice.

44 To date, the majority of biomass pellets are produced from woody biomass due to
45 its high calorific value and low ash content [6]. However, the production of wood-
46 based raw material cannot meet the growing market in demand. It is thus necessary
47 to search for alternative feedstock for biomass pelletization. For non-woody biomass,
48 agricultural waste could be of significant use due to its wide availability and low price.
49 This is especially the case in China, as approximately 0.24 billion tons of corn stover
50 (CS) are produced yearly, accounting for 32% of the total crop residues [7, 8]. Agro-
51 pellets made from corn stover usually have a lower calorific value, a lower density and
52 a higher ash content than that of woody pellets, which can be categorised as a low-
53 grade pellet fuel. There is thus a need to improve the quality of agro-pellets, which can
54 be potentially achieved by pelleting various blends and torrefaction [9, 10]. Previous
55 studies have shown that component complementarity and mechanical interlocking
56 between particles were significantly enhanced through biomass blending [11],
57 consequently leading to a better pelleting performance. For example, Djatkov et al.
58 [12] showed that blending with spruce wood improves the mechanical properties of
59 corn stover pellets. Similar results were reported by Stasiak et al. [3] and Harun et al.
60 [13]. The calorific capacity of straw pellet was found to increase with the addition of
61 higher calorific value pine sawdust. Blending can also reduce compaction energy and
62 thus consumes less energy in the pressing process [13, 14]. In addition to

63 wood/agricultural residues blending, the mixing of various agricultural wastes [15, 16],
 64 co-pelleting of agro-wastes with other residues, such as sewage sludge, pyrolysis oil
 65 and hydrolysis lignin, has also been reported [17-20]. **Table 1** lists a short summary of
 66 biomass blending reported in the literature.

67
 68

Table 1. Blending biomass pellets: literature reviews

Biomass feedstocks	Research objectives	Experimental conclusions	Ref.
Spruce wood and corn stover	The influences on the mechanical-physical properties of corn stover pellets	Blending with wood improved the mechanical properties of corn stover pellets	[12]
Pine sawdust and wheat/ rapeseed straws	Mechanical and combustion properties of pellets made of pine sawdust mixed with straws	Pellet density, strength and calorific capacity increased with the addition of pine sawdust	[3]
Pine sawdust, spruce, timothy hay and switchgrass	The energy requirement for the pelletizing of agricultural biomass	Blending helped to improve the quality of pellets and lower the compaction energy	[13]
Rice husk and wheat straw	Physicochemical and energetic characterization of pellets produced with rice husks and wheat straws	Biomass blends improve the quality and combustion characteristics of the pellets	[16]
Pepper, perilla, rice chaff, and spent coffee	The possibility of pellets made from agricultural by-product	Perilla coffee pellets (PRCP) were determined as A-grade owing to higher durability.	[15]
Sewage sludge and biomass (Chinese fir, camphor and rice straw)	Energy consumption and properties of sludge mixed pellets and pure biomass pellets	Biomass-sludge mixed pellets reduced energy input, increased hardness and improved the combustion characteristics	[20]

69

70 Compared with wood and agricultural wastes and other residues, coal fuel has a
 71 higher calorific value. Heat value and combustion characteristics of argo-pellets can
 72 thus be improved by co-pelleting with coal or coal waste. As the main by-product of
 73 coal mining, coal cutting waste (CCW) is characterised with a high-moisture content

74 and small particle sizes, presenting serious challenges in collection, storage and
75 transportation [21, 22]. For example, in open areas, stored coal cutting waste may
76 pollute ground water and transfer to far places by natural means. Large amounts of
77 unburnt fine particles are released to the atmosphere in the conventional combustion
78 systems, causing environmental problems if they are not controlled properly. In this
79 regard, pelletizing or co-pelletizing allows for an effective use of coal cutting waste [23-
80 25]. Atay and Ekinci [26] characterised the pellets made from lignite coal powder and
81 pine bark. Experimental results showed that the added coal increased combustion
82 temperature and decreased the maximum weight loss rate, leading to an improved
83 combustion efficiency. Janewicz et al. [27] produced pellets from biomass-lignite
84 blends and found that blending pellets present good combustion characteristics but
85 poor water resistance. Both compressive strength and water resistance decreased with
86 the increase of biomass proportion [28]. However, contrary conclusions have been
87 drawn by Yaman et al. [29] and Ozyuguran et al. [30], where the mechanical properties
88 of lignite briquettes were improved by adding biomass while excessive lignite is
89 detrimental to briquetting by decreasing impact resistance and durability of pellets [9,
90 26]. It can thus be concluded that blending with coal or coal waste can improve the
91 calorific value of biomass pellets but may not contribute to the mechanical properties
92 of briquettes. For different biomass and coal materials, it is necessary to provide a
93 guideline on the selection of blending proportion during the co-pelleting process. In
94 this study, torrefied argo-biomass and fine coal particles (coal cutting waste) are
95 selected, with their physical and chemical properties partially changed.

96 In addition to blending with coal cutting waste, torrefaction pre-treatment can
97 improve calorific value and combustion characteristics of argo-pellets [31, 32]. During
98 the torrefaction process, biomass feedstock is heated to the temperature of 200~
99 300 °C with low oxygen concentration [33]. Dehydration breaks large numbers of
100 hydroxyl bonds and reduces hydrogen bonding between biomass and water molecules,
101 consequently improving the hydrophobicity of biomass [34]. With the removal of light
102 volatile fraction that contains most of the oxygen in biomass, heating value of the
103 remaining biomass is gradually increased. Decomposition of hemicellulose destroys
104 the fiber structure of dried biomass, which benefits biomass crushing and improves
105 grinding characteristics [35]. It is worthwhile to note that previous studies are mainly

106 focused on the underlying mechanisms of torrefaction [36, 37] and factors affecting its
107 performance [38] while less attention has been paid to the efficiency of energy
108 utilization for torrefied biomass. This can be readily achieved by life cycle assessment
109 (LCA). Adams et al. [39] assessed torrefaction process in wood pellets production, and
110 found out that torrefied pellets reduced energy consumption: the cumulative energy
111 per kg of modelled torrefied pellets is 18% lower than for the equivalent wood pellets,
112 with primary energy input for torrefied pellets is 43% lower than wood pellets. Rivera
113 et al. [40] identified the energy balance of torrefied microalgal biomass production
114 based on a life cycle approach. The energy analysis showed that torrefaction improves
115 the energy content of the microalgal biomass from 20.22 to 27.93 MJ · kg⁻¹.
116 Torrefaction, among all other scenarios, had the least energy requirement by 20% and
117 less. Lin et al. [41] evaluated the energy return on investment (EROI) to determine the
118 sustainability of torrefied biochar. As the torrefaction temperature increased, EROI
119 index gradually increased from 13.1 to 22.9 for the Ananas comosus peel and from
120 10.9 to 21.9 for the Annona squamosa peel. Fantozzi and Buratti [42] presented a LCA
121 study on household heat from the combustion of wood pellets, where energy return
122 index was calculated. It was reported that energy return index was equal to 3.25 for
123 biomass chain, clearly above the breakpoint, equal to 1. However, for the pellet
124 production process, mass and energy flows were measured on an existing Italian
125 pelleting plant which was completely different from the domestic situation. A number
126 of articles have looked at LCA to quantify and compare the energy performance of
127 biomass pellets, but a wide variation of results can be found in the literature due to
128 the selection of methods, the source of data, the type of raw materials, etc. [43]. In
129 contrast there have only been limited studies which attempt to evaluate the energy
130 efficiency of this innovative argopellets. This paper addresses some of the existing
131 research gaps by performing LCA of upgraded pellets and comparing the results with
132 different processing conditions.

133 It should be noted that mechanical properties and energy efficiency of argo-
134 pellets are still not comparable with that coal particles or wood pellets if upgraded
135 alone by blending or torrefaction. Other processes to improve the utilization level of
136 agricultural waste are still necessary. One of the possible solutions is to combine
137 blending with torrefaction which not only enables a high calorific value and energy

138 efficiency, but it also improves mechanical properties of argo-pellets. Since pelleting is
139 usually operated at high pressure and temperature, more energy is required to
140 increase attractive forces between particles. Si et al. [44] showed that the addition of
141 coal tar is able to improve mechanical durability of biomass pellets at ambient
142 temperature and low pressure. Attempts have also been made to use food waste as
143 binder in engineering applications [45, 46]. For example, starch-rich food waste
144 contributes to granulation, increasing mutual adhesion between particles and
145 consequently reducing energy consumption in pressing and improving the stability of
146 pellets [47]. Although it is feasible in theory, the use of starch-rich food waste as a
147 binder has not been verified experimentally.

148 The objective of this study is to investigate the properties of upgraded argo-pellets
149 manufactured from torrefied corn stover and coal cutting waste, with the use of
150 starch-rich food waster as binder. The effects of coal cutting waste blending, biomass
151 torrefaction and food waste additive on argo-pellets were systematically examined,
152 together with their mechanisms. Experimental conclusions drawn in this work can
153 provide guidelines for argo-pellets optimisation and upgrading in the future.

154

155 **2. Materials and methods**

156 **2.1. Materials**

157 Corn stover used in this study was collected from Henan Province, China. Stover
158 feedstock was washed with distilled water, dried for 36 hours at 105 °C and then
159 ground to powders to ensure a particle size smaller than 2 mm. Torrefaction was
160 conducted in a horizontal sliding tube furnace (TL1200, BYT). After torrefaction at 200 °C
161 for 1.0 hour, the heating furnace was slid back and torrefied corn stover (TCS) was
162 cooled in a quartz tube. Coal cutting waste from a coal processing plant in Anhui
163 Province was used in this experiment. Starch-rich food waste was mainly from bread
164 and pancake, which prepared for the binder after simple cleaning, drying, and grinding.

165 The contents of carbon and hydrogen were quantified by Liebig method (ISO
166 625:1996). Nitrogen concentration was determined by Semi-micro Kjeldahl method
167 (ISO 333:1996). Infrared spectrometry (ISO 19579:2006) was used to quantify the
168 sulfur content, and the remaining oxygen percentage was calculated by the difference
169 according to $O^* = 100 - (C + H + N + S)$. The proximate analysis was referred to GB/T

170 212-2008 standards [48]. According to method ASTM E 711, the calorific value was
 171 determined as the quantity of heat liberated by combustion of a unit quantity of fuel
 172 with oxygen in a standard bomb calorimeter. Three replicates were measured for each
 173 raw material. **Table 2** lists the measured properties of raw materials used in this study.

174

175

Table 2. Ultimate and proximate analysis of CS、TCS and CCW

Parameter	Proximate analysis (wt %, ad.)				Ultimate analysis (wt %, ad.)					Q _{net,ad} (MJ/kg)
	M _{ad}	A	V	FC	C	H	O*	N	S	
CS	7.93	5.98	73.59	12.5	41.57	4.93	52.64	0.66	0.20	13.42
TCS	1.37	6.52	78.18	13.93	46.23	4.49	48.59	0.55	0.14	17.71
CCW	6.66	14.75	30.61	47.98	63.77	3.68	31.24	0.81	0.50	24.34

176

Notes: O*=100%-C-H-N-S; ad: air dry basis

177

178

2.2. Pelletizing process

179

180

181

182

183

184

185

186

187

188

189

Corn stover and coal cutting waste were mixed with the set mass ratios of 9:1, 8:2, 7:3, 6:4 and 5:5. In order to maintain the basic characteristics of argo-pellets, the addition ratio of coal cutting waste was controlled below 50%. Mixture of each proportion was conditioned by adding a fixed amount of starch binder (5% mass), according to the limits of DIN 14961. To compare the effects of starch binder and torrefaction pre-treatment on biomass materials, the other two groups of argo-pellets (one group processed without starch binder and the other group torrefied corn straw) were manufactured at the same blending ratios. These pellets were produced using a laboratory pelletizing unit (PC-10T), made by Tianjin Jingtuo Instrument Technology Co., Ltd, with press channel of 10.0 mm and a diameter of 8.0 mm. The whole pelletizing process is illustrated in **Fig. 1**.



190
191 **Fig. 1.** The pelleting process for pellet samples
192

193 **2.3. Mechanical properties of pellets**

194 The properties of pellet samples were measured according to Pellet Fuel Institute
195 (PFI) Standard (2011). **Fig. 2** illustrates the pellets preparation and analysis processes.
196 The length (L) and diameter (D) of randomly selected biomass pellets were measured
197 with a caliper (CD-56C, Aurora, III). Each measured L and D was recorded to the nearest
198 0.01 mm. True density (TD) was calculated by the ratio of mass to volume. Due to the
199 cylindrical pellet shape, the volume formula was calculated according to the columnar
200 particles. Pellet integrity was established according to the improved PN-G-04651 [49].
201 Pellet samples passed parabolic test (2 m height) and staircase test (14 standard stair
202 face) successively to determine the loss of fine material and undamaged pellets. Then,
203 the pellet integrity was calculated as the percentage of undamaged pellet weight to
204 the total sample weight. Water absorbability was defined by the standard PN-G-04652
205 [49]. Pellet samples were taken out from water for two hours, and then placed in a
206 natural indoor environment for a period of time (3 or 7 days). The difference between
207 the sample weight and the initial weight made the measure of this parameter. The
208 compressive strength and SEM analysis were completed by KC-3 digital particle
209 strength tester and JSM-5610LV scanning electron microscope (SEM), respectively.

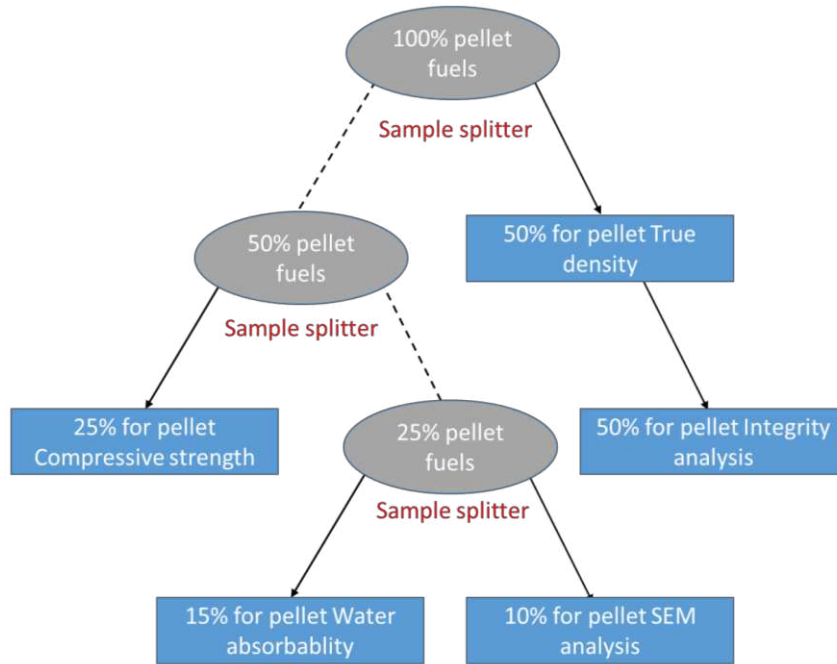


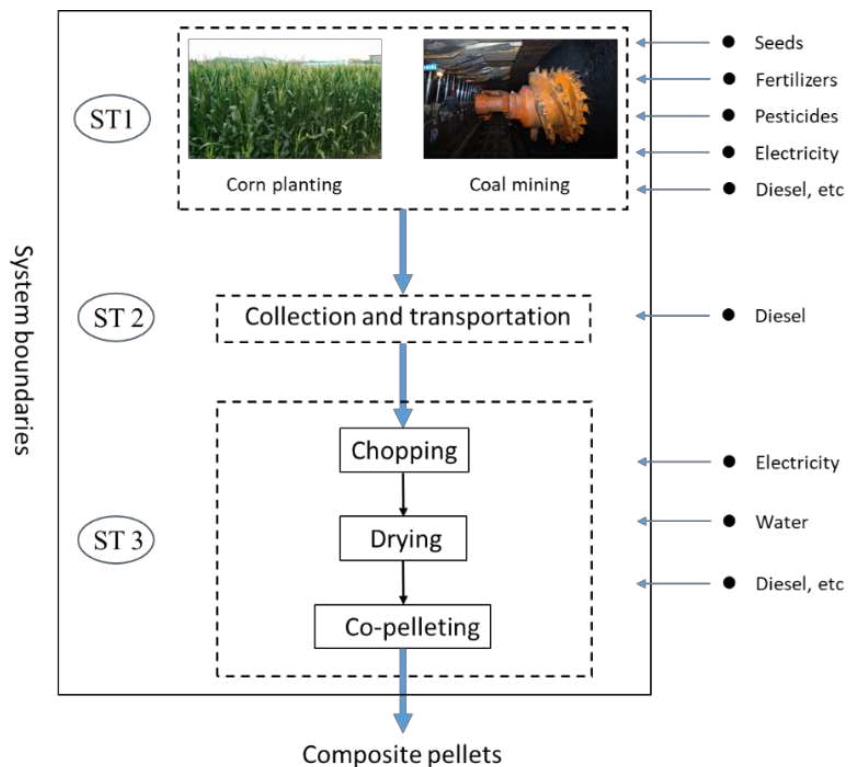
Fig. 2. The flow chart of pellet samples distribution and testing

2.4. Thermal behaviors of pellets

Thermogravimetric/differential thermal analysis (TG/DTA) experiments were performed on a Hitachi synchronous thermal analyzer (STA 449F5®) to characterise thermal properties of samples. In this experiment, 10 ± 0.5 mg material was heated from 25 to 1000 °C at a heating rate of 20 °C/min under 40 mL/min air gas. However, thermogravimetric/mass spectrometry (TG/MS) technique were carried out on Netzsch thermal analyzer (STA 449F3®) coupled with Blazers mass spectrometer (Omnistar 200) to evaluate and characterise of combustion characteristics. In each experiment, 100 mL/min of air gas flow rate and 20 °C/min of heating rate was used from ambient temperature to 1000 °C. Mass spectrometry system was operated under a vacuum and detected the characteristic fragment ion intensity of the volatiles according to respective mass to charge ratios (m/z). The number of m/z signals selected were: 18.03 (H₂O⁺), 30.00 (NO⁺), 43.94 (CO₂⁺), 46 (NO₂⁺), and 63.96 (SO₂⁺). For each experimental process, it was done in triplicate for accuracy and the relative error among all the data was controlled within 5%. After all the experiments, thermal data was derived and processed by Origin 8.5 to obtain multiple thermodynamic curves to compare the combustion difference of different pellet fuels.

231 **2.5. Life cycle assessment of pellets**

232 This study aims to quantitatively assess the quality of argo-pellets by life cycle
 233 assessment (LCA) meanwhile exploring the feasibility of upgrading argo-pellets. Energy
 234 Return Ratio (ERR) is the ratio of the amount of usable energy obtained from a
 235 resource to the amount of energy expended to produce that net amount of energy
 236 [50]. The larger the ERR, the greater the net energy output and the higher the energy
 237 efficiency. In this study, the reference functional unit was selected as one-ton pellet
 238 fuel production. The corresponding calorific value was measured with a standard
 239 bomb calorimeter. Energy input of production equipment, plant, land and living
 240 facilities are not considered. The upstream production data of the material is also
 241 ignored, as raw material weight is less than 5%. In addition, waste and disposal are
 242 excluded from the boundary. **Fig. 3** presents the system boundary for pellets
 243 production, including three key stages which are: corn planting and coal mining (ST1);
 244 feedstocks collection and transportation (ST2); and pellet fuels production (ST3:
 245 chopping, drying, and co-pelleting).



246

247

Fig. 3. The diagram of system boundary of pellets production

248

249

Table 3 presents the inventory data for corn planting stage per functional unit,

250 without considering output to technosphere. The consumption of raw materials is
 251 mainly collected from the calculated results of Henan statistical yearbook and
 252 literature [51]. Some necessary background data, such as the generation and
 253 transportation of raw materials, are derived from Ecoinvent 3.1 database, which is
 254 representative of China. As an agricultural waste, the yield of corn stover is 1.2 times
 255 of corn while its price is one tenth of corn. Based on the principle of economic
 256 distribution [51], the proportion of energy consumption in corn planting allocated to
 257 corn and corn stover are 90% and 10%, respectively. For coal mining, the relevant
 258 energy input data and background data are derived from similar reference [52]. The
 259 second stage (ST2) is the collection and transportation of raw material. According to
 260 the previous study [51], the average collection distance from fuel plant to corn planting
 261 area is set as 15 km, and the distance between fuel plant and coal area is about 50 km.
 262 Feedstocks are transported by the third-party trucks (Dongfeng, 8t load capacity), with
 263 average diesel consumption of 0.15 L/km and load factor of 50%. The last process (ST3)
 264 combines chopping, drying, and co-pelleting. Long corn stover is first crushed and
 265 dried, and then sprayed with water to adjust the water content approximate 10%
 266 before co-pelleting with dried coal cutting waste. Electricity is mainly consumed by
 267 drying machine, chopping device, and pelleting machine. For torrefied biomass, the
 268 power consumption includes vacuum torrefaction equipment. The natural loss and
 269 lifespan of various mechanical equipment are not considered in the LCA calculation.
 270 The consumed water, electricity, diesel, etc. are calculated according to actual pellets
 271 processing plant in Henan province, which are listed in **Table 4**.

272

273 **Table 3..** Inventory data for corn planting per functional unit (1t pellets)-ST1

Item	Total Amount	Unit	Corn	Corn stover
Nitrogen fertilizer (N urea)	15.78	kg	14.2	1.58
Phosphate fertilizer (P ₂ O ₅)	8.844	kg	7.96	0.884
Potassium fertilizer (K ₂ O)	6.722	kg	6.05	0.672
Pesticides	0.789	kg	0.71	0.079
Electricity	36.4	kWh	32.76	3.64

Diesel	10.9	L	9.81	1.09
--------	------	---	------	------

274

275 **Table 4..** Inventory data for pellet fuels production per functional unit (1t pellets) –ST2 and ST3

Item	Amount	Unit	Description
Corn stover	1100	kg	Used for raw material, loss rate of the whole process is about 10%
Diesel (Collection and transportation)	0.306	L	Corn stover collection and transportation
Electricity-Drying	32.7	kWh	JTSG1415, Electricity consumption during drying
Electricity-Chopping	2.5	kWh	HY-400, Electricity consumption during chopping
Electricity-Torrefaction	34.87	kWh	HY-8, Electricity consumption during torrefaction
Electricity-Pelleting	93.4	kWh	RGKJ560, Electricity consumption during pelleting
Water	22.77	kg	Water spraying in pellets production
Diesel (In-plant transportation)	0.12	L	For transportation of material and pellet fuels

276

277 **3. Results and discussion**

278 The photo of manufactured pellet fuels under different process conditions are
 279 presented in **Fig. 4**. As feedstocks are pressed by machine, the particle size of pellets
 280 is generally maintained, with a length of 8 mm and a diameter of 10 mm. Most of the
 281 briquette fuels exhibit excellent formability and integrity, and the color of pellets
 282 changes obviously: with an increase of CCW mixing ratio, the color of pellet fuels
 283 deepens. Moreover, the color of torrefied pellets (TCS+CCW+5%S) is obviously darker
 284 than that of pellets without torrefaction (CS+CCW and CS+CCW+5%S). Theoretically,
 285 the darker the color, the higher the calorific value, but this needs to be verified by
 286 combustion experiments. The effect of starch-food binder on pellets cannot be
 287 identified directly, hence further physical test and analysis are required.

288

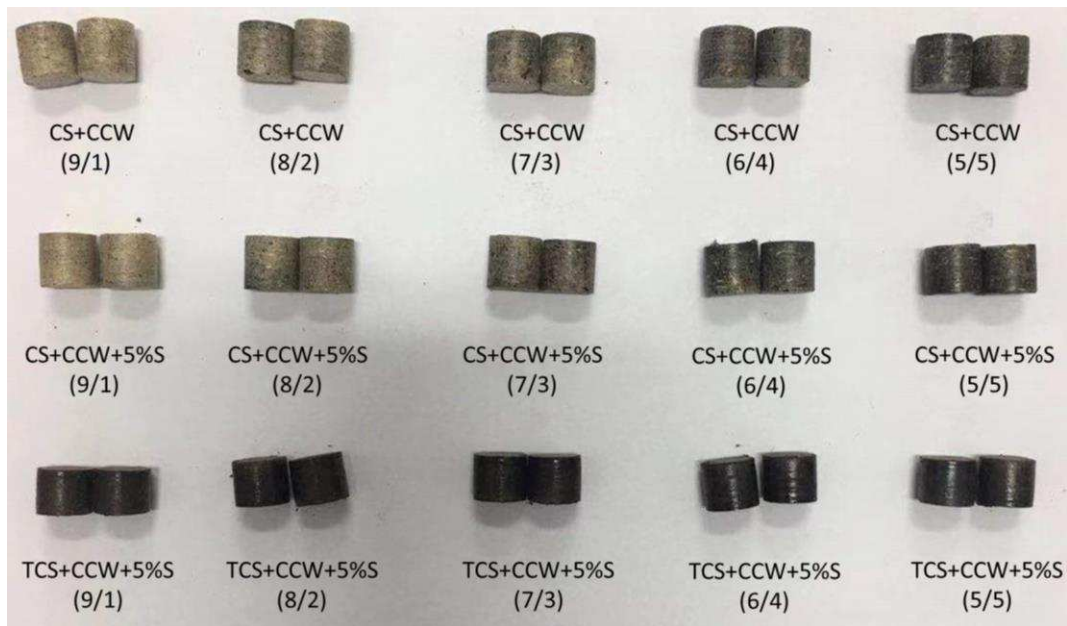


Fig. 4. Pellet fuels under different experimental conditions (CS: corn straw; TCS: torrefied corn straw; CCW: coal cutting waste; S: starch-binder)

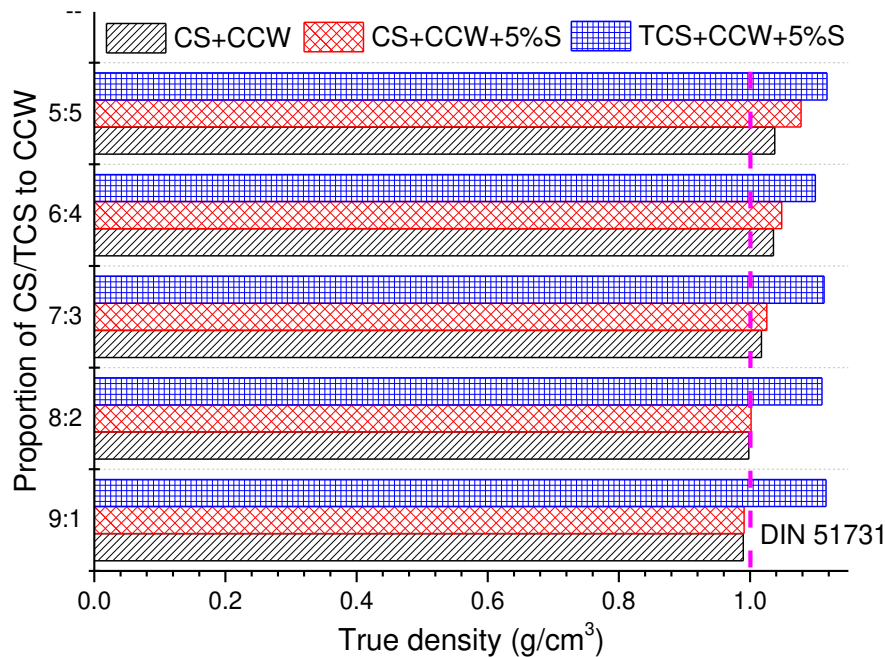
3.1 Mechanical properties

3.1.1 True density

True density is an important parameter for pellet fuels, calculated as the ratio of mass to volume of single pellet. A large true density corresponds to a high transport efficiency and a small storage space [53]. **Fig. 5** presents the true densities of various pellet fuels. It is obvious that the pellet densities (CS+CCW and CS+CCW+5%S) increase with CCW percentage. The reason can be attributed to the higher density of CCW than that of CS. For torrefied corn stover (TCS), the advantage of high-density CCW is not that obvious. **Fig. 5** indicates that pellet density (TCS+CCW+5%S) remains nearly unchanged with the addition of CCW. However, the density of torrefied pellets (TCS+CCW+5%S) is much higher than that without torrefaction. Basically, all pellet fuels can meet the DIN 51731 standard (i.e., 1000 kg/m³), except for CS pellets blending with 10% CCW. However, once 10% CCW is mixed with TCS, the pellet density is much higher than 1000 kg/m³ as a result of torrefaction.

The addition of starch binder has a positive impact on pellet density, which is obvious when the CS fraction is less than 70%. The improvement on pellet density is more obvious with further decrease of CS proportion. In contrast, as the proportion of CS is 80% or 90% in **Fig. 5**, the addition of starch binder has little influence on true

311 density. Previous studies have shown that lignin was the main component of self-
 312 binding in stover, which combined with cellulose and hemicellulose to produce pellets
 313 by intermolecular attraction and entanglement [54, 55]. It may be speculated that the
 314 external starch binder plays the main role in palletization with less CS, and the internal
 315 lignin binder will gradually act with increasing CS. However, relevant inferences and
 316 assumptions need to be verified in future studies.



317
 318 **Fig. 5.** Pellet true density as related to CS/TCS to CCW and starch binder addition (CS: corn straw;
 319 TCS: torrefied corn straw; CCW: coal cutting waste; S: starch-binder)

320

321 3.1.2 Pellet integrity

322 **Fig. 6** shows that with increasing CCW percentage, the pellet integrity increases
 323 first and then decreases. The maximum value of integrity is found at a mixing ratio of
 324 (8:2) between CS and CCW. Blending different feedstocks can improve pellet integrity,
 325 and similar conclusions was also drawn in previous study [56]. Compared with CS, the
 326 particle size of CCW is much smaller. The addition of a small amount of CCW fills the
 327 gap between CS particles, which contributes to the improvement of pellet forming and
 328 integrity. This is especially so for CS without torrefaction. For instance, when CCW
 329 blending ratio increases from 10% (9CS:1CCW) to 20% (8CS:2CCW), the pellet integrity
 330 is improved by 1% (from 98.2% to 99.2%). In the presence of starch binder
 331 (CS+CCW+5%S), particle size is not the only factor affecting pelleting. The integrity of

332 mixed pellets (TCS+CCW+5%S) remains nearly unchanged while the physicochemical
333 properties of torrefied biomass are modified, and the effect of particle size is
334 significantly reduced.

335 Overall, the pellet fuels meet the DIN 1496 class-A requirement (97.5% for
336 integrity). The pellet integrity after torrefaction (TCS+CCW+5%S) is higher than that
337 without torrefaction (CS+CCW+5%S) and the pellet integrity with starch binder
338 (CS+CCW+5%S) is better than that without starch binder (CS+CCW). Corn straw
339 contains chemical extractives, such as low molecular weight fatty acids, waxes, sterols
340 and terpenes [57]. When CS material is milled, these chemical substances migrate to
341 particle surface and thus hinders the binding of CS molecules. This phenomenon is
342 called passivation which reduces compression strength and integrity of pellets, as
343 confirmed by Bergstrom et al. [58]. After torrefaction treatment, some of these
344 chemical extractives from CS can be removed, thus reducing this passivation effect.
345 This is the reason for the high pellet integrity of pellet fuels (TCS+CCW+5%S). Starch
346 binder mainly includes dextrin, cellulose, free sugar, and pentosan, which plays an
347 important role in pelleting process. The internal forces of pelleting includes attractive
348 force, interfacial force, capillary force, adhesive and cohesive forces, solid bridges of
349 particles [59]. Liu et al. [56] found that the predominant bonding was created by solid
350 bridges during palletization. Adding starch additive can strengthen these solid bridges
351 and promote pellet formation. Clearly, the effect of starch binder is dependent on the
352 mixing ratio of CS and CCW. In **Fig. 6**, with the decrease of CS mixing ratio, the positive
353 effect of starch on integrity is reduced. Even when the proportion of CS is 50%, the
354 addition of starch binder reduces pellet integrity. This may be related to the reaction
355 between starch binder and the components of CS or CCW, resulting in synergy or
356 antagonism.

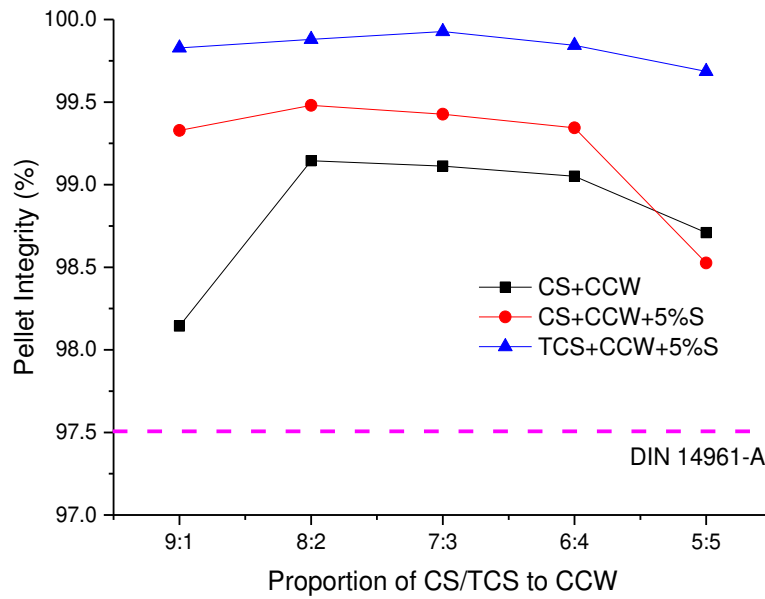
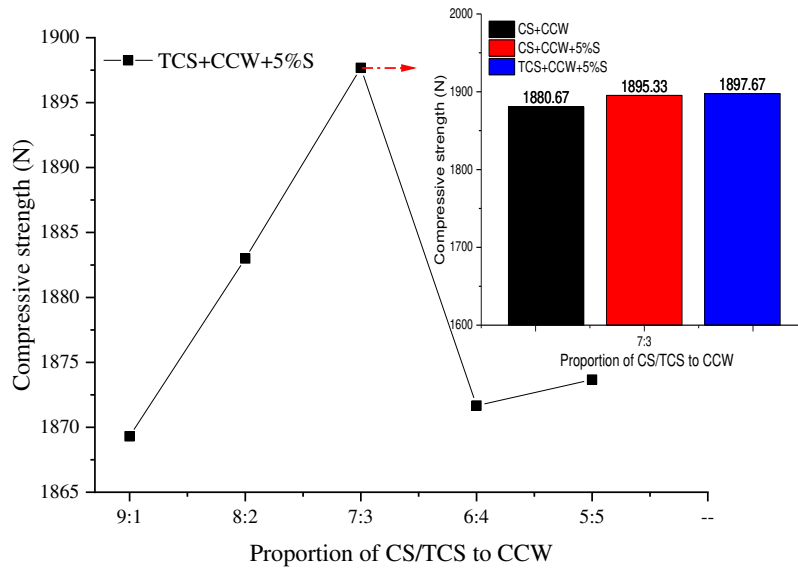


Fig. 6. Pellet integrity as related to CS/TCS to CCW and starch addition (CS: corn straw; TCS: torrefied corn straw; CCW: coal cutting waste; S: starch-binder)

3.1.3 Compressive strength

Similar to pellet integrity, the compressive strength of pellets rises first and then falls, as shown in **Fig. 7**. When the mixing ratio of TCS is 70%, the pellet fuel has the maximum compressive strength of 1897.67 N/cm². The addition of starch binder also improves the compressive strength from 1880.67 to 1895.33 N/cm². However, the effect of torrefaction is extremely weak, and the compressive strength remains largely stable, from 1895.33 to 1897.67 N/cm². SEM results in **Fig. 8** show that the surface of unroasted pellets has an obvious layered structure, mainly due to the spiral extrusion in channel. The material without starch binder (CS+CCW) has rough surface, loose texture and a small amount of gap and pore structures. After the addition of starch-binder, the layered structures (CS+CCW+5%S) are more obvious, orderly, and compact. This structural difference caused by starch-binder is the main reason for the improvement of pellet integrity and compressive strength. Torrefied granular fuel (TCS+CCW+5%S) still contains layered structures, but the layered structures are interspersed with partial melting and crosslinking, resulting in the reduction of intermittent space and the enhancement of compactness. This may be the reason why torrefied pellets have greater integrity and compressive strength.



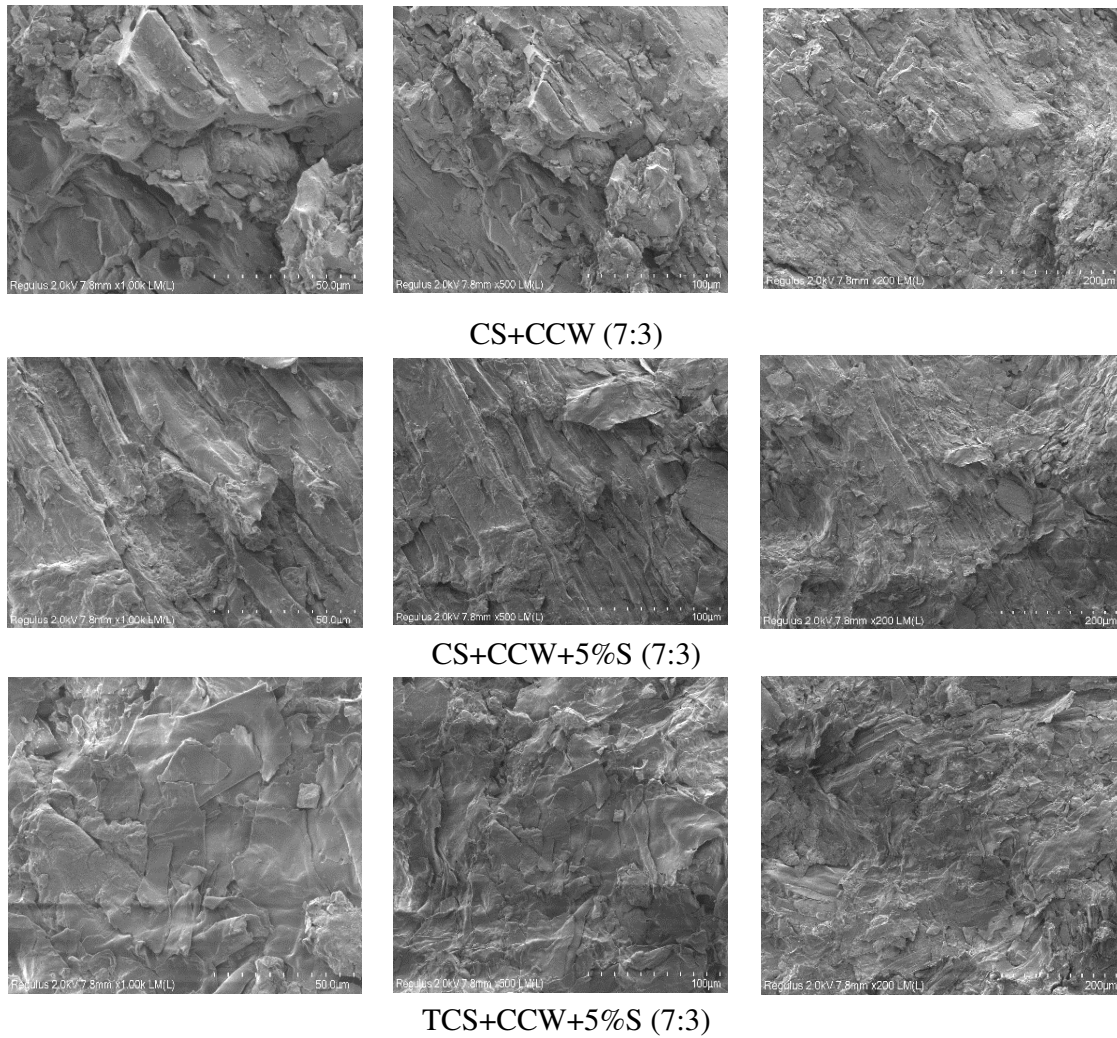
378

379

Fig. 7. Compressive strength as related to CS/TCS to CCW and starch addition (CS: corn straw;

380

TCS: torrefied corn straw; CCW: coal cutting waste; S: starch)



381

382

Fig. 8. SEM of pellets (CS: corn straw; TCS: torrefied corn straw; CCW: coal cutting waste; S:

383

starch)

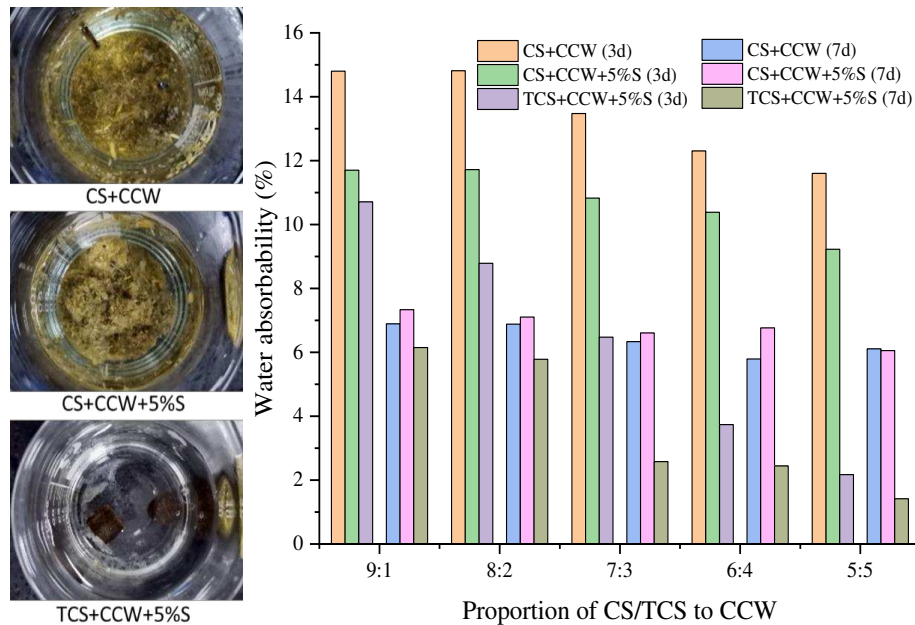
384

385 **3.1.4 Water absorbability**

386 Regardless of whether starch binder is added or not, pellet fuels without
387 torrefaction decompose obviously after soaking in water for 24 hours as shown in **Fig.**
388 **9**, indicating that their water resistance stabilities are relatively poor. On the contrary,
389 the torrefied fuel presents good water resistance and still has high integrity after
390 soaking for a period of time. This is mainly related to the composition of CS material.
391 Hemicellulose in corn straw is rich in hydroxyl groups, which are the main groups of
392 water absorption [20]. After torrefaction, the hydroxyl groups of corn straw are
393 decomposed by heating, which weakens the water absorption function. In addition,
394 the surface of torrefied particles contains some hydrophobic organic matters [20],
395 which can further reduce the water absorption.

396 The water absorbability of pellet fuels is closely related to the weak bond
397 between particles and the corresponding pore structure. **Fig. 9** plots water
398 absorbability of pellet fuels versus CS/TCS proportion. The water absorption decreases
399 gradually with decreasing proportion of CS (from 90% to 50%). Moreover, water
400 absorption of torrefied pellets (TCS+CCW+5%S) was much less than that of the non-
401 torrefied pellets. The presence of starch binder (CS+CCW+5%S) leads to a smaller
402 water absorption than that without starch (CS+CCW). Torrefaction heating destroys
403 some hydroxyl groups; therefore, the water absorption is weakened. The addition of
404 starch binder during pelleting process improves the mechanical strength and reduces
405 the pore structures between particles. In general, the above two mechanisms of
406 reducing water absorption are essentially different. The effect of time on the decrease
407 of water absorption is further investigated. It was found that the water absorption of
408 pellet fuels decreases differently with times from 3 to 7 days. Among them, the water
409 absorption of pellets without starch-binder (CS+CCW) decreases the most up to 40~
410 50%, and the decline seems to be related to the proportion of CS. When the CS
411 percentage is the highest, the largest decline is obtained. Moreover, a smaller decrease
412 is observed at a lower CS ratio, which is mainly due to the role of hemicellulose in CS.
413 This difference shows that the hydroxyl weak bond is unstable and easy to be affected
414 by external environment. Different from the function of hydroxyl bond, starch-binder
415 mainly acts instantaneously. With the increase of time, water absorption

416 (CS+CCW+5%S) decreases, with a reduction range smaller than that without binder
 417 (CS+CCW) and a minor influence due to the ratio of CS. In comparison, pellet fuels with
 418 the smallest water absorption corresponds to a TCS proportion of 50%, implying that
 419 torrefaction greatly improves water resistance and stability of pellet fuels.



420
 421 **Fig. 9.** Pellet water absorbability as related to CS/TCS to CCW and starch addition (CS: corn straw;
 422 TCS: torrefied corn straw; CCW: coal cutting waste; S: starch)

424 3.2 Thermal behaviors

425 3.2.1 TG-DTG-DTA

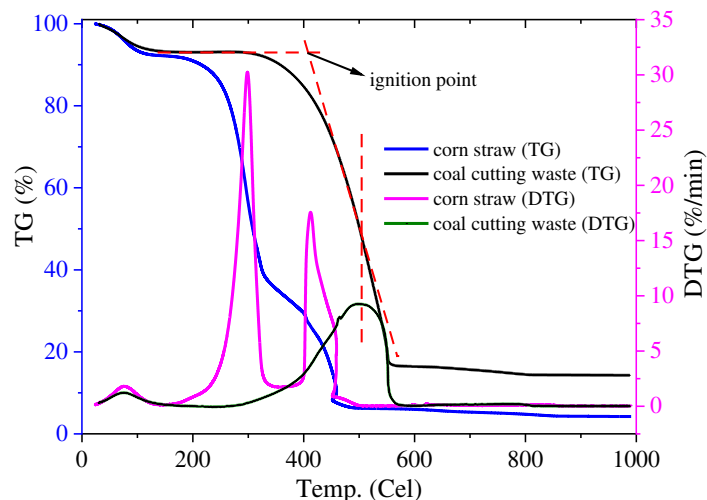
426 Thermogravimetric analysis is an efficient method widely used for the analysis of
 427 combustion process [60]. **Fig. 10** shows the thermal profiles of CS and CCW. The weight
 428 loss of CS can be observed in three main stages: first) the dehydration and drying stage
 429 ranged from 80 °C to 160 °C; second) the pyrolysis of lignin and cellulose, and the
 430 release of volatile matter starting from 160 °C and finishing at 370 °C and third) coke
 431 combustion took place between 370 and 470 °C. The first weight-loss stage is mainly
 432 due to the evaporation of water molecules. The second stage represents the loss of
 433 CO, and the third stage of weight-loss is mainly caused by volatilisation of CO₂. The
 434 final stage was characterised by a slight weight loss, which is mainly caused by the
 435 further cracking of C-C and C-H bonds. Three weightlessness peaks can be observed
 436 from the DTG curves, with the volatile release-combustion peak much larger than the
 437 peak of fixed char combustion. This is mainly because the volatile matter of CS is much

438 greater than its fixed char, thus showing a higher rate of release and combustion.

439 The weight loss of CCW combustion can be divided into two stages: dehydration
440 (90 ~ 220 °C), and volatile release and fixed char combustion (220 ~ 580 °C). The first
441 step is weaker than that of CS as the moisture content of CCW is lower than that of CS.
442 The second weight-loss step is related to fixed char, where the weight loss increases
443 with fixed char in CCW. There are two weightlessness peaks on the DTG curves:
444 dehydration peak and the peak of volatile release-combustion and fixed char
445 combustion. Due to the low volatile content and high volatile release temperature of
446 CCW (390 ~ 500 °C), the volatile release-combustion peak of CCW is not fully reflected.
447 The volatile release and combustion are always accompanied by the combustion of
448 coal char. There is only one obvious weight loss peak except the dehydration peak on
449 the DTG curves.

450 By comparing the DTG curves of CS and CCW, it can be seen that the combustion
451 process of CS is mainly concentrated in the volatile combustion stage while the
452 combustion process of CCW is mainly concentrated in the fixed carbon combustion
453 stage. Different from the sharp combustion peaks of CS, the volatile release and fixed
454 char combustion peak of CCW shows a shoulder peak.

455



456

457

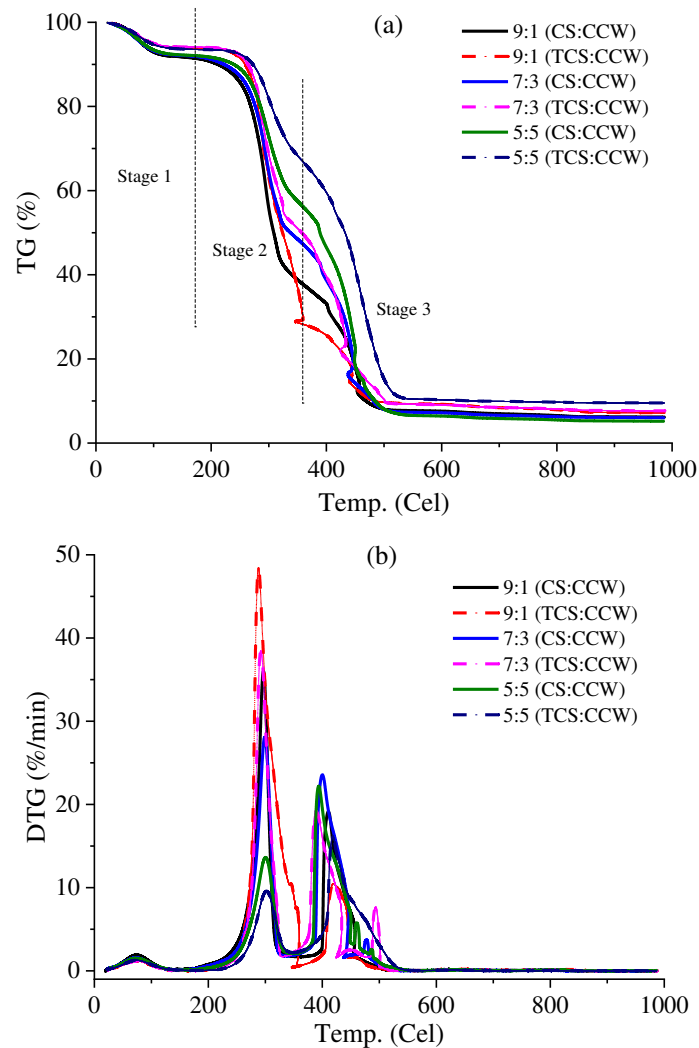
Fig. 10. TG and DTG curves of corn straw/coal cutting waste

458

459 It can be observed that TG and DTG curves of CS/TCS and CCW blends are
460 arranged in order according to the proportion of feedstocks. As shown in **Fig. 11(a)**,
461 the same first peak is obtained for both, this might be due to the dehydration of

462 moisture from 80 to 160 °C. Note that the dehydration stage is not analysed here. The
463 combustion process mainly consists of two stages: volatile release-combustion and
464 fixed char combustion. TG curves of blends basically coincide when the temperature
465 is lower than 120 °C while differs with a temperature over 120 °C. With the increase
466 of CCW ratio, TG curves move towards the high temperature zone, and the ignition
467 temperature (T_i) and burnout temperature (T_b) of the mixtures rise gradually, as shown
468 in **Table 4**. In addition, the weakening of the second weight loss step is more
469 pronounced due to a low volatile content of CCW, and the third step is gradually
470 enhanced due to a higher fixed carbon content of CCW than that of CS. Comparing TG
471 curves with or without torrefaction treatment, the second weight loss step is
472 weakened after pre-treatment, indicating that torrefaction is conducive to pyrolysis
473 and volatile precipitation. Torrefaction improves the fuel performance of biomass,
474 mainly reflected in the improvement of moisture content, fixed carbon content, and
475 energy density. Torrefaction had a significant impact on the distribution and
476 characteristics of biomass pyrolysis products. The increase of pyrolysis carbon from
477 torrefied biomass was mainly due to the large decomposition of hemicellulose and the
478 sharp increase of lignin content, while the lignin pyrolysis products were mainly
479 biochar.

480 According to DGT curves shown in **Fig. 11(b)**, the greater the CS proportion in the
481 mixtures, the higher the volatile content, and the greater peak value of volatile release
482 and combustion. Theoretically, the lower the CCW ratio in the mixtures, the lower the
483 fixed carbon content and the smaller peak value of coke combustion. However, the
484 coke combustion peak is the highest ($D_{max}=23.5$ mg/min) when the ratio is 7:3 (CS:
485 CCW). Feedstocks with high carbon content can continuously provide higher heat for
486 the combustion process, so as to promote the combustion of fixed carbon or residual
487 samples. Meanwhile, raw materials with high ash content are easy to generate ash
488 shell during burnout stage, which hinders the inward infiltration of oxygen and the
489 outward diffusion of combustion products. The calorific value of CCW is large, but the
490 ash content is also high. Therefore, only selecting the appropriate mixing proportion
491 can help to improve the burnout characteristics of blending pellets.



492

493

494 **Fig. 11.** TG and DTG curves of CS/CCW and TCS/CCW at different ratios (CS: corn straw; TCS:
495 torrefied corn straw; CCW: coal cutting waste)

496

497 The peak values of volatile release and combustion increases after torrefaction as
498 shown in **Table 5**. This is mainly due to the increase of calorific value of torrefied CS.
499 Torrefied CS combustion preheats CCW and promotes the release of volatile matters,
500 which is conducive to pellets ignition and burnout. However, when the CCW mixing
501 ratio was larger (at 50%), the decrease of DGT peak is not conducive to the overall
502 combustion, which is also related to the high ash content from CCW.

503 DTA curves with exothermic and endothermic areas are presented in **Fig. 12**,
504 which are similar to mass loss trend of TG curves. By integrating the area under DTA
505 curves, the heat release from the entire combustion process can be obtained to
506 understand the thermodynamic behavior. Experimental results showed that the
507 calorific value of pellet fuel can be improved by mixing with CCW (from 13540.8 to

508 19467.1 J/g) and torrefaction pretreatment (from 13973.8 to 18659.1 J/g, from
 509 17271.6 to 19264.1 J/g, from 19467.1 to 23049.3 J/g). The corresponding interval of
 510 exothermic is devolatilization or combustion (stage 2) and fixed char combustion
 511 (stage 3). The endothermic peak is mainly caused by the endothermic volatilization of
 512 moisture.

513 **Table 5.** The combustion characteristics of pellet fuels

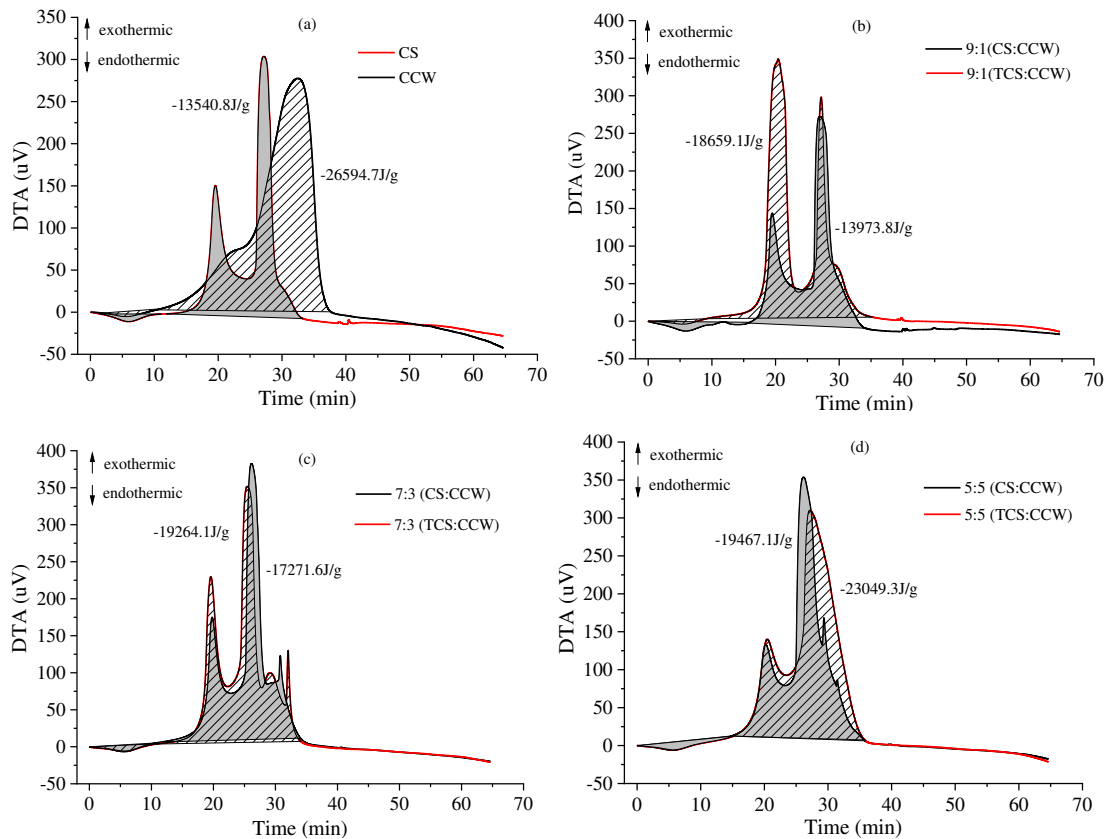
Samples	Volatile release and Combustion				Char combustion			T_b (°C)
	T_i	T_p	D_{max}	M	T_p	D_{max}	M	
	(°C)	(°C)	(mg/min)	(%)	(°C)	(mg/min)	(%)	
CS	252	299	30.2	58.1	406	17.4	26.8	505
9:1(CS:CCW)	258	299	35.9	53.7	412	19.0	30.5	518
9:1(TCS:CCW)	261	290	48.2	47	420	10.4	18.9	529
7:3(CS:CCW)	261	300	28	43.4	402	23.5	42.3	534
7:3(TCS:CCW)	260	294	38.2	41	390	19	36.1	545
5:5(CS:CCW)	265	300	13.6	34.6	392	22	52.4	585
5:5(TCS:CCW)	274	302	9.5	25.4	420	16.3	58	599
CCW	408	—	—	—	502	9.2	76.5	650

514 Notes: T_i = ignition temperature; T_p = peak temperature; D_{max} = the highest combustion peak; M = mass ratio; T_b =
 515 burnout temperature.

516

517 Obviously, the heat peak of pure CS is higher at char combustion stage than that
 518 at the volatile combustion stage with a ratio of 2, indicating more heat is released per
 519 unit weight during coke combustion. Compared with CS combustion, the CCW peaks
 520 in the whole DTA curves are smoother in **Fig. 12(a)**. Similar conclusions have been
 521 drawn by previous studies [49, 61]. Theoretically, with the addition of CCW, the
 522 thermal profiles of CS/CCW will become smoother, as the desired result of combustion
 523 of fuel mixtures [48, 62]. **Figs. 12(a)-(d)** demonstrated that the addition of CCW
 524 smoothed CS thermal curves, but the effect was very limited. Moreover, when the
 525 CCW blending ratio is 30%, the DTA peak of CS/CCW reaches the maximum value of
 526 380 μ V, which may be related to the synergistic effect of CS and CCW [48]. Compared
 527 with original CS, the torrefied CS increased the DTA peak of volatile combustion and
 528 decreased the peak of char combustion, and the whole thermal curve tended to be
 529 smoother. In other words, the combustion of TCS/CCW presents relatively small

530 difference in heat distribution. The use of fuels with small differences in heat
 531 distribution curves can improve the availability of the boiler in operation.



532

533

534 **Fig. 12.** DTA curves of CS/TCS and CCW at different ratios (a=CS/CCW; b=9:1; c=7:3; d=5:5)

535

536 3.2.2 TG-MS

537 **Fig. 13** presents the variation of ion current of various gaseous components with
 538 temperature at the same heating rate of 20 °C/min. Moisture vaporised at about 100 °C
 539 and displayed a good ion peak as shown in **Fig. 13(a)**. The mass evaporation of water
 540 mainly occurred within the temperature range of 200 to 400 °C, corresponding to the
 541 volatilization stage[63]. For different pellet fuels, the largest H₂O peak is observed for
 542 pure CS, reaching 3.8×10^{-9} A/mg. Because the water content of CCW (6.66%) is
 543 slightly lower than that of CS (7.93%), when they are mixed up to produce the new
 544 blending pellets (0.7CS:0.3CCW), there is a slight decrease in H₂O peak. Similarly, after
 545 torrefaction treatment, the moisture ratio of CS decreases sharply (1.37%) and the H₂O
 546 peak of blending pellets (0.7TCS:0.3CCW) is the smallest. Biomass is mainly composed
 547 of cellulose, hemicellulose and lignin, and their contents affect the moisture release
 548 process directly. Hemicellulose begins to decompose and release water molecule

549 approximately at 200 °C, while the temperature for cellulose and lignin is higher, about
550 250 °C [64]. However, most of water was lost after torrefaction, thereby the H₂O peak
551 is not very prominent compared with the case without torrefaction.

552 The CO₂ ion profiles are distributed in the entire combustion process, as shown
553 in **Fig. 13(b)**. Two prominent peaks of CO₂ can be found between 200 and 600 °C, which
554 are attributed to the decomposition of anhydrides, phenols, quinones, carbonates,
555 carbonyls and ethers [65]. Note that there is a slightly different peak in the range of
556 600 to 800 °C. This indicates that carbonates or covered carbon in ash is decomposed
557 at high temperatures during combustion. For different pellet fuels, it is obvious that
558 both blending CCW and biomass torrefaction shift the curve towards right, implying
559 that a higher burnout temperature is required for fuels burnout. This change is mainly
560 related to the increase of carbon content in pellet fuel, which would consequently
561 cause an increase in carbon dioxide emission.

562 Fuel nitrogen mainly exists in the form of gaseous nitrogen, tar nitrogen and char
563 nitrogen. The main products in volatilization stage are volatile nitrogen and char
564 nitrogen, in which volatile nitrogen is composed of gaseous nitrogen and tar nitrogen.
565 Gaseous nitrogen (NH₃, HCN, HNCO) can be further converted to NO, in which partial
566 NO is oxidised to NO₂, or N₂ is generated under the reduction of hydrocarbons and
567 coke. At high temperature, char nitrogen is further oxidised through combustion
568 reaction to produce NO and NO₂ [66].

569 Elemental analysis in **Table 2** shows that the content of nitrogen in CCW is greater
570 than that in CS. In theory, the combustion of CS mixed with CCW will release more
571 nitrogen compounds. However, when the temperature is low (<400°C), nitrogen
572 mainly exists in the form of gas-phase volatiles, and CS itself contains more volatile
573 components, thereby it presents a very obvious large NO peak in **Fig. 13(c)**. With the
574 increase of temperature, a relatively gentle NO peak appears on the CS curve, which
575 is because most of the nitrogen precipitates in the form of volatiles and a small amount
576 exists in char. In the temperature range of 400 °C - 650 °C, the content of char nitrogen
577 in CCW is higher, and presents an obvious NO peak compared with CS. When the
578 temperature reaches about 650 °C, the ion current of NO and NO₂ increase briefly in
579 **Fig. 13(c) and(d)**, respectively. A portion of nitrogen-containing compounds exited as
580 the nitrate or covered organic in CS and CCW [63]. As the temperature rises, nitrogen-

581 containing compounds decomposes to form nitrogen oxides (NO₂ and NO). Meanwhile,
582 NO₂ is reduced to NO on the coke surface at high temperature. It can be confirmed by
583 **Fig. 13(d)** that the concentration of NO₂ decreases significantly at the same
584 temperature. When the temperature is higher than 700 °C, the higher the carbon
585 content, the more carbon reacts with NO₂ and the more NO is generated. Compared
586 with the raw material CS, CCW blending and torrefaction both can improve the carbon
587 content of pellet fuel.

588 During combustion, the formation of sulfur oxides is related to the occurrence
589 form, temperature and composition of sulfur. In the devolatilization stage, sulfur
590 oxides mainly come from organic sulfur, and sulfur oxides are mainly the
591 decomposition of inorganic sulfur during char combustion. As shown in **Fig. 13(e)**, SO₂
592 gas is mainly produced in the volatiles release and combustion stage. Due to the low
593 sulfur content in CS, there is only a weak SO₂ peak at 300 - 500 °C, and the
594 corresponding peak value is 5.0×10^{-13} A/mg. The sulfur proportion of CCW is 2.5 times
595 that of CS, thereby the SO₂ emission peak of co-combustion of CS and CCW is very
596 sharp (1.5×10^{-12} A/mg). Heating during torrefaction can remove some sulfur-
597 containing organic matter in the form of volatiles, resulting in the reduction of sulfur
598 content in pellet fuel, and the SO₂ released by combustion is greatly reduced ($8.5 \times$
599 10^{-13} A/mg).

600 The total gas emission during combustion is calculated by integral method. The
601 cumulative amount of different gas products is shown in **Fig. 13(f)**. As the main gas
602 composition of all pellet fuels, the total amount of H₂O and CO₂ accounts for more
603 than 99% of the total gas products. The co-combustion of CS and CCW leads to the
604 increase of CO₂ and NO₂ emissions, which is mainly due to the high proportion of C
605 and N in CCW. Although the emissions of CO₂ and NO₂ per unit mass increases, the
606 emission of pollutants with the same calorific value will be greatly reduced due to co-
607 combustion. After torrefaction treatment, the content of C element in CS increased,
608 the content of N and S elements decreased, and the element compositions of raw
609 material changed significantly. Meanwhile, the release of NO and SO₂ are reduced in
610 the gas accumulation diagram. Although the CO₂ emission increased, the calorific
611 value of pellet fuel (TCS+CCW) was improved. The results showed that torrefaction

612 technology was conducive to reduce the pollutant emissions and significantly improve
 613 the quality of raw materials.

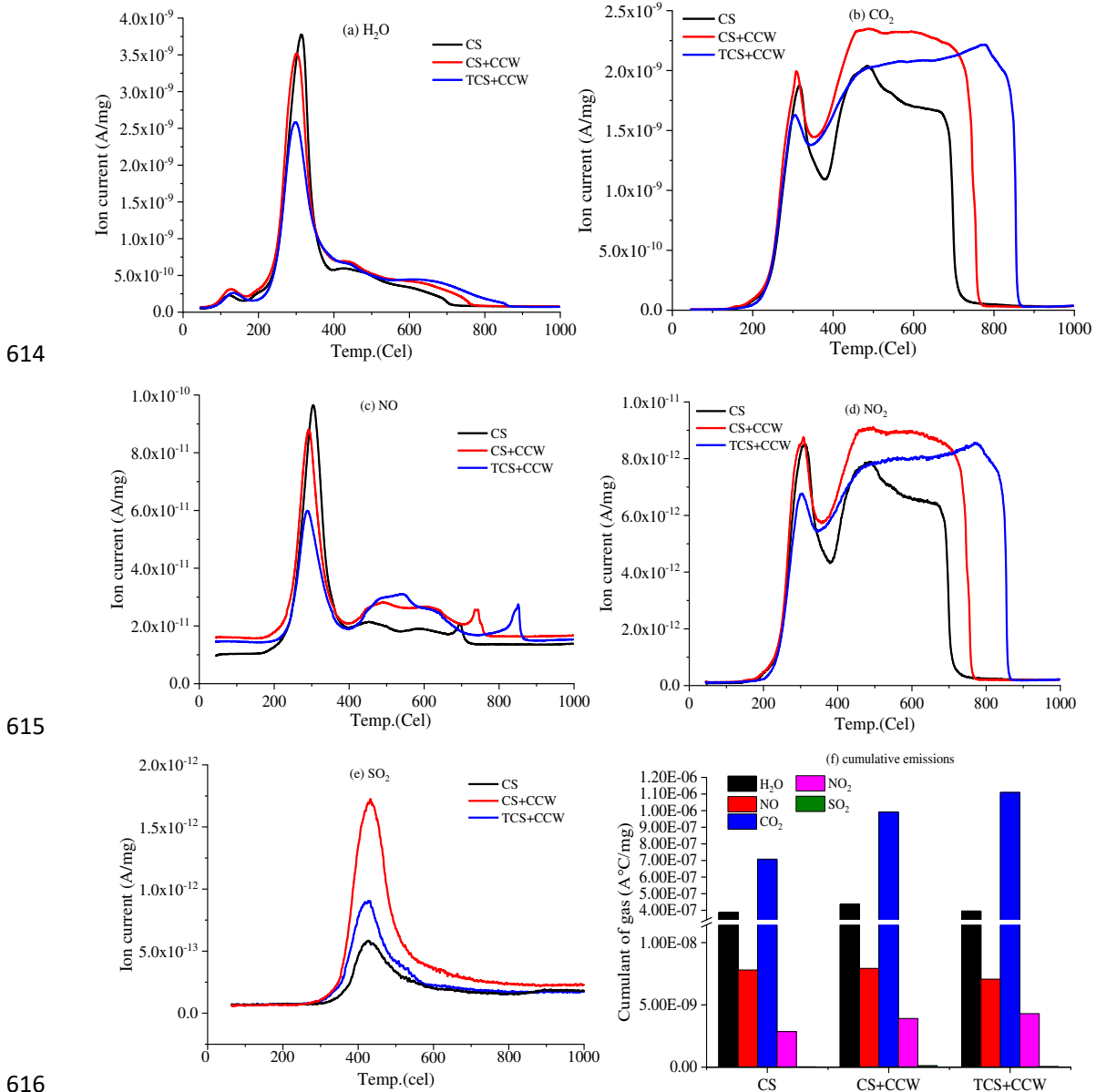


Fig. 13. Gas emission curves of(a) H₂O, (b) CO₂, (c) NO, (d) NO₂ (e) SO₂ and (f) cumulative emissions at the heating rate of 20 °C/min

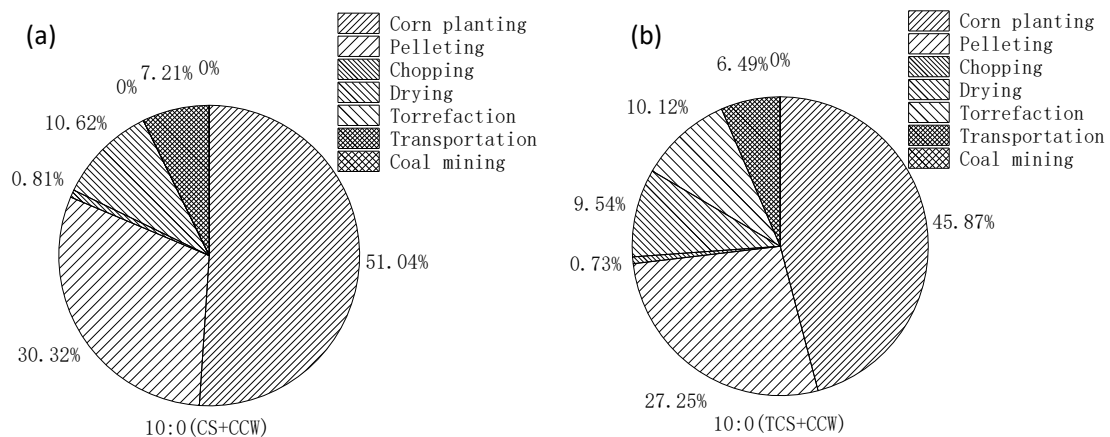
3.3 LCA analysis

The energy input in the whole life cycle of pellet fuel manufacturing is shown in **Fig. 14**. For pure biomass pellet (CS and TCS), energy input is mainly used for corn planting, accounting for 51.04% (10CS:0CCW) and 45.87% (10TCS:0CCW), respectively; the second is the pressing processing of pellet fuel, with energy consumption accounting for 27.25 - 30.32%. These results are in line with those previously reported

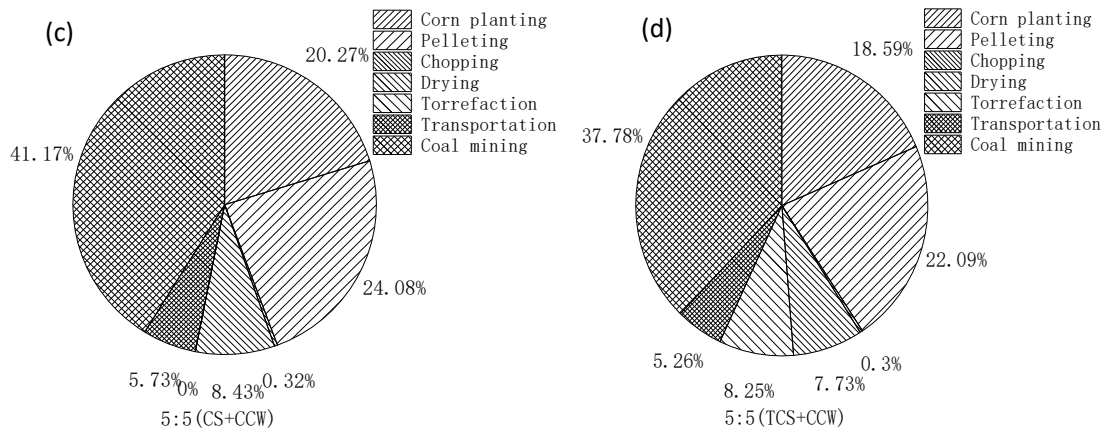
626 by Hamedani et al. [50], where biomass cultivation and pelletizing were reported as
 627 the main contributors to energy consumption in olive pellet production. It is also clear
 628 that transportation and chopping are the least consuming energy activities.
 629 Torrefaction process is the main power consumption, accounting for about 10.12% of
 630 the total energy input, as shown in **Fig. 14(b)**. For biomass pellet fuel blending with
 631 CCW, the top three energy consumption are coal mining (37.78 - 41.17%), pellet
 632 pressing (22.09 - 24.08%), and corn planting (18.59 - 20.27%). Similar to biomass pellet,
 633 the composite pellet fuel consumes less energy in the transportation and chopping
 634 processes, consistent with previous studies [42, 50]. The mixing amount of CCW
 635 directly affects the total energy input. Therefore, a reasonable selection of CCW
 636 blending proportion is critical for energy efficiency of pellet fuel.

637 **Fig. 15** shows that EER increases slowly with CCW blending ratio. Although increasing
 638 CCW leads to an increase in the total input energy, a higher calorific value of CCW
 639 implies a larger total output heat, thereby showing a better performance of EER.
 640 Moreover, the energy efficiency of pellet fuel improves with torrefaction, with the EER
 641 increases in varying degrees. However, this extent of improvement depends on the
 642 proportion of biomass material, which is more significant at large proportions of
 643 biomass.

644

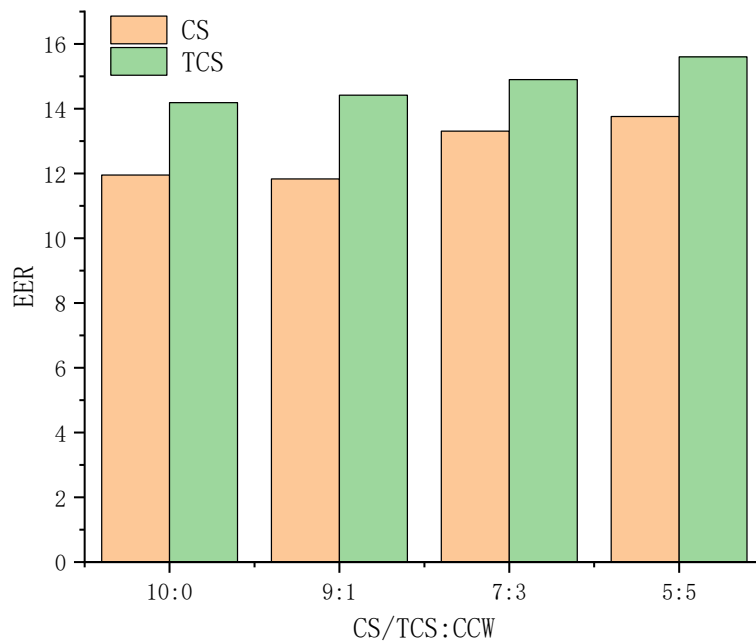


645



646
647
648
649

Fig. 14. Comparison of cumulative energy demand in pellet fuel production (a) 10CS:0CCW, (b) 10TCS:0CCW, (c) 5CS:5CCW, (d) 5TCS:5CCW



650
651
652

Fig. 15. Energy Return Ratio of different pellet fuel samples

653 3.3 Discussion and future perspectives

654 Combining the above-mentioned research findings, a summary of the physical
655 and combustion characteristics of upgraded argo-pellets has been presented in **Fig. 16**.
656 There are two feasible ways to improve the quality of argo-pellets: mixing CCW and
657 torrefaction. Mechanical properties: with increasing CCW percentage, all the physical
658 parameters increases, except that the pellet integrity increases first and then
659 decreases. The addition and use of starch can further optimise this physical

660 performance. CS torrefaction can improve these mechanical properties in varying
 661 degrees on the basis of starch addition and CCW mixing. In terms of compressive
 662 strength, the compressive performance of argo-pellets first increases and then
 663 decreases, reaching the maximum at 30% mixing ratio of CCW. Combustion
 664 characteristics: CCW blending and torrefaction both improve the thermodynamic
 665 characteristic parameters, release more calorific value and present higher energy
 666 efficiency. However, C, N and S account for a large proportion in CCW, and the simple
 667 blending is not conducive to environmental protection. Although torrefaction
 668 treatment increases the proportion of C, it releases more net heat energy and reduces
 669 the contents of N and S. From the perspective of unit energy output, it is conducive to
 670 the emission reduction of pollutants.

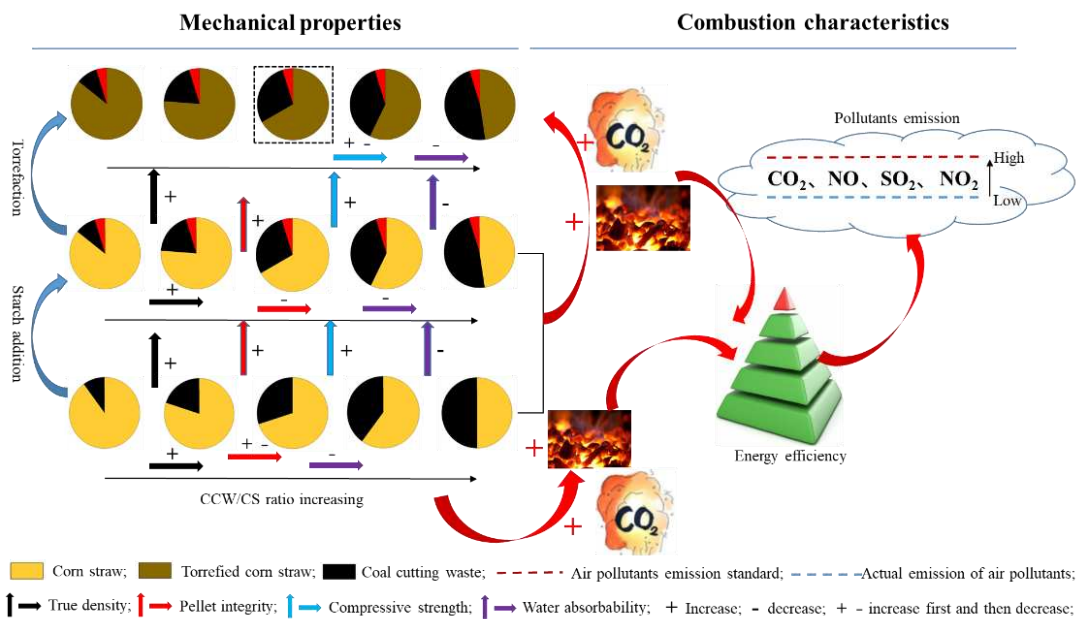


Fig. 16. The variation of mechanical and combustion characteristics of upgraded argo-pellets under different processing conditions

675 Considering that biomass itself belongs to clean energy, the blending of biomass
 676 and CCW to upgrade the quality of argo-pellets is still a feasible scheme on the premise
 677 of meeting the emission standards of air pollutants. However, in some places with high
 678 requirements for pollutant emission, the combination of torrefaction treatment and
 679 reduced proportion of CCW blending needs to be adopted. Based on the mechanical
 680 properties and combustion characteristic parameters of argo-pellets, the proportion

681 of CCW blending recommended in this study is 30%. For different sources of
682 agricultural and coal waste, the recommended blending proportion may be changed.
683 Meanwhile, the emission standards of air pollutants are often aimed at the emission
684 of biomass or coal, and lack of relevant blending pellets. Therefore, future studies need
685 to pay more attention to the variation of raw materials and the formulation of
686 pollutant emission standards. In addition, LCA study in this work does not consider the
687 main pollutant emission (CO₂) during the whole process, and the corresponding
688 environmental impact analysis needs to be added in the follow-up, so as to analyse the
689 pollutant emission in the whole process more comprehensively. CS and CCW are two
690 different forms of waste; and upgraded argo-pellets show a good market prospect. The
691 resource combined utilisation of these two wastes is a promising method with high
692 economic benefits.

693

694 **4. Conclusions**

695 This work aimed to improve the quality of argo-pellets by blending with CCW,
696 torrefaction treatment and adding starch binder. On the basis of the obtained results
697 and discussion, the main conclusions can be drawn as:

- 698 • Mechanical experiments showed that co-pelleting of TCS and CCW with starch
699 binder was technically possible. The qualities of the pellet samples including
700 true density, pellet integrity, compressive strength and water absorbability
701 have been improved to varying degrees.
- 702 • Thermogravimetric analysis revealed that the appropriate proportion of less
703 CCW can not only promote the combustion of blending pellets, but also
704 improve the thermodynamic characteristic parameters of torrefied pellet.
705 Compared with CCW blending, torrefaction treatment can more effectively
706 smooth the DTA curves, which improves the availability for the boiler in
707 operation.
- 708 • Both CCW blending and torrefaction can reduce the concentration of NO_x and
709 SO₂, improve the calorific value of fuel, but increase the CO₂ emission per unit
710 mass. Comprehensive considering the increase of calorific value and CO₂
711 emission, co-combustion and torrefaction are conducive to pollutants

712 reduction and improve the quality of raw materials
713 • LCA analysis indicated that increasing the blending ratio of CCW and
714 torrefaction pre-treatment requires more energy input, but the energy
715 efficiency EER of pellet fuel will also be improved.

716

717 **Declaration of competing interest**

718 The author declares no competing financial interest.

719

720 **Acknowledgements**

721 The authors are grateful to the support given by the Youth Projects of Jiangsu
722 Natural Science Foundation (BK20200736 and BK20190704), the National Natural
723 Science Foundation of China (No. 52106094), Natural Science Foundation of the Higher
724 Education Institutions of Jiangsu Province (20KJB610007), and the Program for High-
725 Level Entrepreneurial and Innovative Talents Introduction of Jiangsu Province
726 (202030488).

727

728 **References**

- 729 [1] S.W. Yu, Y.M. Wei, H.X. Guo, L.P. Ding. Carbon emission coefficient measurement of the coal-to-power
730 energy chain in China. *Appl Energ.* 114 (2014) 290-300.
- 731 [2] H. Bloch, S. Rafiq, R. Salim. Economic growth with coal, oil and renewable energy consumption in
732 China: Prospects for fuel substitution. *Econ Model.* 44 (2015) 104-15.
- 733 [3] M. Stasiak, M. Molenda, M. Banda, J. Wiacek, P. Parafiniuk, E. Gondek. Mechanical and combustion
734 properties of sawdust-Straw pellets blended in different proportions. *Fuel Process Technol.* 156
735 (2017) 366-75.
- 736 [4] E. Alakoski, M. Jamsen, D. Agar, E. Tampio, M. Wihersaari. From wood pellets to wood chips, risks of
737 degradation and emissions from the storage of woody biomass - A short review. *Renew Sust Energ*
738 *Rev.* 54 (2016) 376-83.
- 739 [5] L.J.R. Nunes, J.C.O. Matias, J.P.S. Catalao. A review on torrefied biomass pellets as a sustainable
740 alternative to coal in power generation. *Renew Sust Energ Rev.* 40 (2014) 153-60.
- 741 [6] N. Mansuy, E. Thiffault, S. Lemieux, F. Manka, D. Pare, L. Lebel. Sustainable biomass supply chains
742 from salvage logging of fire-killed stands: A case study for wood pellet production in eastern Canada.
743 *Appl Energ.* 154 (2015) 62-73.
- 744 [7] X.Y. Wang, L. Yang, Y. Steinberger, Z.X. Liu, S.H. Liao, G.H. Xie. Field crop residue estimate and
745 availability for biofuel production in China. *Renew Sust Energ Rev.* 27 (2013) 864-75.
- 746 [8] L.L. Zhao, X.M. Ou, S.Y. Chang. Life-cycle greenhouse gas emission and energy use of bioethanol
747 produced from corn stover in China: Current perspectives and future perspectives. *Energy.* 115
748 (2016) 303-13.

- 749 [9] M.V. Gil, P. Oulego, M.D. Casal, C. Pevida, J.J. Pis, F. Rubiera. Mechanical durability and combustion
750 characteristics of pellets from biomass blends. *Bioresource Technol.* 101 (2010) 8859-67.
- 751 [10] S. Yu, J. Park, M. Kim, H. Kim, C. Ryu, Y. Lee, et al. Improving Energy Density and Grindability of
752 Wood Pellets by Dry Torrefaction. *Energy Fuel.* 33 (2019) 8632-9.
- 753 [11] H. Li, L.B. Jiang, C.Z. Li, J. Liang, X.Z. Yuan, Z.H. Xiao, et al. Co-pelletization of sewage sludge and
754 biomass: The energy input and properties of pellets. *Fuel Process Technol.* 132 (2015) 55-61.
- 755 [12] D. Djatkov, M. Martinov, M. Kaltschmitt. Influencing parameters on mechanical-physical properties
756 of pellet fuel made from corn harvest residues. *Biomass Bioenerg.* 119 (2018) 418-28.
- 757 [13] N.Y. Harun, A.M. Parvez, M.T. Afzal. Process and Energy Analysis of Pelleting Agricultural and Woody
758 Biomass Blends. *Sustainability-Basel.* 10 (2018).
- 759 [14] R. Garcia, M.V. Gil, F. Rubiera, C. Pevida. Pelletization of wood and alternative residual biomass
760 blends for producing industrial quality pellets. *Fuel.* 251 (2019) 739-53.
- 761 [15] S. Park, S.J. Kim, K.C. Oh, L. Cho, M.J. Kim, I.S. Jeong, et al. Investigation of agro-byproduct pellet
762 properties and improvement in pellet quality through mixing. *Energy.* 190 (2020).
- 763 [16] I.M. Rios-Badran, I. Luzardo-Ocampo, J.F. Garcia-Trejo, J. Santos-Cruz, C. Gutierrez-Antonio.
764 Production and characterization of fuel pellets from rice husk and wheat straw. *Renew Energ.* 145
765 (2020) 500-7.
- 766 [17] A.A. Siyal, Y. Liu, X. Mao, Z.A. Siyal, C.M. Ran, W.Y. Ao, et al. Co-pelletization of sewage sludge,
767 furfural residue and corn stalk: Characteristics and quality analysis of pellets. *Biomass Bioenerg.*
768 150 (2021).
- 769 [18] W.Z. Li, W.J. Bu, W.W. Guo, Y. Jiang, A. Wang, X.L. Yin. Preparation for industrial pellet production
770 from blends of eucalyptus sawdust and hydrolysis lignin: the optimal variable combinations of co-
771 pelletization. *Biomass Convers Bior.* 10 (2020) 513-21.
- 772 [19] T.R. Sarker, R. Azargohar, A.K. Dalai, V. Meda. Characteristics of torrefied fuel pellets obtained from
773 co-pelletization of agriculture residues with pyrolysis oil. *Biomass Bioenerg.* 150 (2021).
- 774 [20] L.B. Jiang, X.Z. Yuan, Z.H. Xiao, J. Liang, H. Li, L. Cao, et al. A comparative study of biomass pellet
775 and biomass-sludge mixed pellet: Energy input and pellet properties. *Energy Convers Manage.* 126
776 (2016) 509-15.
- 777 [21] M. Rejdak, J. Robak, A. Czardybon, K. Ignasiak, P. Fudala. Research on the Production of Composite
778 Fuel on the Basis of Fine-Grained Coal Fractions and Biomass-The Impact of Process Parameters
779 and the Type of Binder on the Quality of Briquettes Produced. *Minerals-Basel.* 10 (2020).
- 780 [22] D.P. Patil, D. Taulbee, B.K. Parekh, R. Honaker. Briquetting of Coal Fines and Sawdust - Effect of
781 Particle-Size Distribution. *Int J Coal Prep Util.* 29 (2009) 251-64.
- 782 [23] M. Sawadogo, S.T. Tanoh, S. Sidibe, N. Kpai, I. Tankoano. Cleaner production in Burkina Faso: Case
783 study of fuel briquettes made from cashew industry waste. *J Clean Prod.* 195 (2018) 1047-56.
- 784 [24] J.J. Hu, T.Z. Lei, Z.W. Wang, X.Y. Yan, X.G. Shi, Z.F. Li, et al. Economic, environmental and social
785 assessment of briquette fuel from agricultural residues in China - A study on flat die briquetting
786 using corn stalk. *Energy.* 64 (2014) 557-66.
- 787 [25] P. Dinesha, S. Kumar, M.A. Rosen. Biomass Briquettes as an Alternative Fuel: A Comprehensive
788 Review. *Energy Technol-Ger.* 7 (2019).
- 789 [26] O.A. Atay, K. Ekinici. Characterization of pellets made from rose oil processing solid wastes coal
790 powder/pine bark. *Renew Energ.* 149 (2020) 933-9.
- 791 [27] A. Janewicz, B. Kosturkiewicz, A. Magdziarz. Briquetting lignite-biomass blends to obtain composite
792 solid fuels for combustion purposes. *Iop C Ser Earth Env.* 214 (2019).

- 793 [28] A. Janewicz, B. Kosturkiewicz. Preparation of fuel briquettes composite made of lignite and biomass.
794 Przem Chem. 94 (2015) 1521-3.
- 795 [29] S. Yaman, M. Sahan, H. Haykiri-Acma, K. Sesen, S. Kucukbayrak. Fuel briquettes from biomass-lignite
796 blends. Fuel Process Technol. 72 (2001) 1-8.
- 797 [30] A. Ozyuguran, H.H. Acma, E. Dahiloglu. Production of fuel briquettes from rice husk-lignite blends.
798 Environ Prog Sustain. 36 (2017) 742-8.
- 799 [31] N. Kienzl, N. Margaritis, R. Isemin, V. Zaychenko, C. Strasser, D.S. Kourkoumpas, et al. Applicability
800 of Torrefied Sunflower Husk Pellets in Small and Medium Scale Furnaces. Waste Biomass Valori. 12
801 (2021) 2579-96.
- 802 [32] N. Margaritis, P. Grammelis, E. Karampinis, I.P. Kanaveli. Impact of Torrefaction on Vine Pruning's
803 Fuel Characteristics. J Energ Eng. 146 (2020).
- 804 [33] S. Negi, G. Jaswal, K. Dass, K. Mazumder, S. Elumalai, J.K. Roy. Torrefaction: a sustainable method
805 for transforming of agri-wastes to high energy density solids (biocoal). Rev Environ Sci Bio. 19 (2020)
806 463-88.
- 807 [34] W. Yan, T.C. Acharjee, C.J. Coronella, V.R. Vasquez. Thermal Pretreatment of Lignocellulosic Biomass.
808 Environ Prog Sustain. 28 (2009) 435-40.
- 809 [35] W.H. Chen, P.C. Kuo. Torrefaction and co-torrefaction characterization of hemicellulose, cellulose
810 and lignin as well as torrefaction of some basic constituents in biomass. Energy. 36 (2011) 803-11.
- 811 [36] M.J.C. van der Stelt, H. Gerhauser, J.H.A. Kiel, K.J. Ptasinski. Biomass upgrading by torrefaction for
812 the production of biofuels: A review. Biomass Bioenerg. 35 (2011) 3748-62.
- 813 [37] W.H. Chen, J.H. Peng, X.T.T. Bi. A state-of-the-art review of biomass torrefaction, densification and
814 applications. Renew Sust Energ Rev. 44 (2015) 847-66.
- 815 [38] Y.Q. Niu, Y. Lv, Y. Lei, S.Q. Liu, Y. Liang, D.H. Wang, et al. Biomass torrefaction: properties, applications,
816 challenges, and economy. Renew Sust Energ Rev. 115 (2019).
- 817 [39] P.W.R. Adams, J.E.J. Shirley, M.C. McManus. Comparative cradle-to-gate life cycle assessment of
818 wood pellet production with torrefaction. Appl Energy. 138 (2015) 367-80.
- 819 [40] D.R.T. Rivera, A.T. Ubando, W.H. Chen, A.B. Culaba. Energy balance of torrefied microalgal biomass
820 with production upscale approached by life cycle assessment. J Environ Manage. 294 (2021).
- 821 [41] Y.L. Lin, N.Y. Zheng, C.H. Hsu. Torrefaction of fruit peel waste to produce environmentally friendly
822 biofuel. J Clean Prod. 284 (2021).
- 823 [42] F. Fantozzi, C. Buratti. Life cycle assessment of biomass chains: Wood pellet from short rotation
824 coppice using data measured on a real plant. Biomass Bioenerg. 34 (2010) 1796-804.
- 825 [43] M. Martin-Gamboa, P. Marques, F. Freire, L. Arroja, A.C. Dias. Life cycle assessment of biomass
826 pellets: A review of methodological choices and results. Renew Sust Energ Rev. 133 (2020).
- 827 [44] T.T. Si, J. Cheng, F. Zhou, J.H. Zhou, K.F. Cen. Control of pollutants in the combustion of biomass
828 pellets prepared with coal tar residue as a binder. Fuel. 208 (2017) 439-46.
- 829 [45] G. Borowski, W. Stepniewski, K. Wojcik-Oliveira. Effect of starch binder on charcoal briquette
830 properties. Int Agrophys. 31 (2017) 571-4.
- 831 [46] Z.X. Wang, Y.B. Zhai, T.F. Wang, B. Wang, C. Peng, C.T. Li. Pelletizing of hydrochar biofuels with
832 organic binders. Fuel. 280 (2020).
- 833 [47] J.S. Tumuluru, C.C. Conner, A.N. Hoover. Method to Produce Durable Pellets at Lower Energy
834 Consumption Using High Moisture Corn Stover and a Corn Starch Binder in a Flat Die Pellet Mill.
835 Jove-J Vis Exp. (2016).
- 836 [48] F.H. Guo, Y. He, A. Hassanpour, J. Gardy, Z.P. Zhong. Thermogravimetric analysis on the co-

837 combustion of biomass pellets with lignite and bituminous coal. *Energy*. 197 (2020).

838 [49] M. Wzorek, R. Junga, E. Yilmaz, P. Niemiec. Combustion behavior and mechanical properties of
839 pellets derived from blends of animal manure and lignocellulosic biomass. *J Environ Manage*. 290
840 (2021).

841 [50] S.R. Hamedani, A. Colantoni, F. Gallucci, M. Salerno, C. Silvestri, M. Villarini. Comparative energy
842 and environmental analysis of agro-pellet production from orchard woody biomass. *Biomass
843 Bioenerg*. 129 (2019).

844 [51] Z.W. Wang, T.Z. Lei, M. Yang, Z.F. Li, T. Qi, X.F. Xin, et al. Life cycle environmental impacts of cornstalk
845 briquette fuel in China. *Appl Energ*. 192 (2017) 83-94.

846 [52] L. Huo, Y. Tian, H. Meng, L. Zhao, Z. Yao. LIFE CYCLE ASSESSMENT ANALYSIS FOR DENSIFIED BIOFUEL.
847 *Acta Energiæ Solaris Sinica*. 32 (2011) 1875-80.

848 [53] B. Lehmann, H.W. Schroder, R. Wollenberg, J.U. Repke. Effect of miscanthus addition and different
849 grinding processes on the quality of wood pellets. *Biomass Bioenerg*. 44 (2012) 150-9.

850 [54] J.E.G. van Dam, M.J.A. van den Oever, E.R.P. Keijsers, J.C. van der Putten, C. Anayron, F. Josol, et al.
851 Process for production of high density/high performance binderless boards from whole coconut
852 husk - Part 2: Coconut husk morphology, composition and properties. *Ind Crop Prod*. 24 (2006) 96-
853 104.

854 [55] J.M. Castellano, M. Gomez, M. Fernandez, L.S. Esteban, J.E. Carrasco. Study on the effects of raw
855 materials composition and pelletization conditions on the quality and properties of pellets obtained
856 from different woody and non woody biomasses. *Fuel*. 139 (2015) 629-36.

857 [56] Z.J. Liu, X.E. Liu, B.H. Fei, Z.H. Jiang, Z.Y. Cai, Y. Yu. The properties of pellets from mixing bamboo
858 and rice straw. *Renew Energ*. 55 (2013) 1-5.

859 [57] E.L. Back. Oxidative Activation of Wood Surfaces for Glue Bonding. *Forest Prod J*. 41 (1991) 30-6.

860 [58] M. Stehr, I. Johansson. Weak boundary layers on wood surfaces. *J Adhes Sci Technol*. 14 (2000)
861 1211-24.

862 [59] N. Kaliyan, R.V. Morey. Natural binders and solid bridge type binding mechanisms in briquettes and
863 pellets made from corn stover and switchgrass. *Bioresource Technol*. 101 (2010) 1082-90.

864 [60] S.S. Idris, N.A. Rahman, K. Ismail. Combustion characteristics of Malaysian oil palm biomass, sub-
865 bituminous coal and their respective blends via thermogravimetric analysis (TGA). *Bioresource
866 Technol*. 123 (2012) 581-91.

867 [61] M. Mureddu, F. Dessi, A. Orsini, F. Ferrara, A. Pettinau. Air- and oxygen-blown characterization of
868 coal and biomass by thermogravimetric analysis. *Fuel*. 212 (2018) 626-37.

869 [62] F.H. Guo, Z.P. Zhong. Co-combustion of anthracite coal and wood pellets: Thermodynamic analysis,
870 combustion efficiency, pollutant emissions and ash slagging. *Environ Pollut*. 239 (2018) 21-9.

871 [63] T. Wang, T.M. Fu, K. Chen, R.S. Cheng, S. Chen, J.X. Liu, et al. Co-combustion behavior of dyeing
872 sludge and rice husk by using TG-MS: Thermal conversion, gas evolution, and kinetic analyses.
873 *Bioresource Technol*. 311 (2020).

874 [64] W.H. Chen, C.W. Wang, H.C. Ong, P.L. Show, T.H. Hsieh. Torrefaction, pyrolysis and two-stage
875 thermodegradation of hemicellulose, cellulose and lignin. *Fuel*. 258 (2019).

876 [65] Z.H. Yuan, Y.Y. Shen, H.P. Yuan, A.M. Sui, N.W. Zhu, Z.Y. Lou. A collaborative approach to in-situ
877 oxysulfides and oxynitrides fixation in flue gas and energy recycling: Co-combustion of spent
878 bleaching earth and coal. *J Clean Prod*. 258 (2020).

879 [66] F.H. Guo, Z.P. Zhong. Experimental studies on combustion of composite biomass pellets in fluidized
880 bed. *Sci Total Environ*. 599 (2017) 926-33.